

# A Novel Hybrid Islanding Detection Technique in Multi DG Microgrid System



Shashank Gupta, Santosh Kumar Singh, and Mahiraj Singh Rawat

## 1 Introduction

The best option for supplying the continuous energy of world needs is the solution as green energy (GE) source as opposed to burning fossils. The continuous degrading of fossil fuels has detrimental effects on the ecosystem and accelerates temp of environment lead to globally wide spread warming. For such of these cause, the world is looking to renewable energy sources (RES), VU/THD, and bilateral reactive power variation to satisfy future energy demands [1]. Therefore, the green energy generating units like solar with wind and hydro refers to small-scale power generating projects that are most likely to be integrated to the grid. The most serious issue with DG systems, though, is islanding. From the standards referred by IEEE 1547 [2], “An island represents a state where segment of an area aka electric power system (EPS) is powered by one or more locally supported EPSs with their associated PCCs and that segment of EPS is electrically isolated from rest of the left out EPS”. Term islanding can be mainly categorizes in according to state of act ion i.e.: happened unintentionally and next is done for any particular purpose also known as intentional islanding. During intentionally isolating a microgrid from the main grid, it continues to reliably provide power energy support to local loads. It’s a controllable mode of operation. When microgrids are cut off from the main grid, inadvertent islanding happens as a result of line tripping, failure, and human error. Some disrupting utility infrastructure on the main grid are major highlighted drawbacks of islanding which accidently or unintentionally occurred includes danger to working personal at work. Identification for non-intendant islanding, many islanding detection techniques (IDTs)

---

S. Gupta (✉) · S. K. Singh · M. S. Rawat  
Department of Electrical Engineering, National Institute of Technology, Uttarakhand, Srinagar  
(Garhwal), India  
e-mail: [mt20eee012@nituk.ac.in](mailto:mt20eee012@nituk.ac.in)

© The Author(s), under exclusive license to Springer Nature Singapore Pte Ltd. 2023  
S. Doolla et al. (eds.), *Advances in Renewable Energy and Its Grid Integration*,  
Lecture Notes in Electrical Engineering 1041,  
[https://doi.org/10.1007/978-981-99-2283-3\\_7](https://doi.org/10.1007/978-981-99-2283-3_7)

are categorized and proposed by researchers in literature. IDTs can further be classified: local and remote techniques. Communication between a utility and DGs has been supported by remote IDTs. The reliability of these techniques performs better than local methods, but they are not much economical. For the most of instances at distributed generation (DG) side, the locally evaluated parameter calculative techniques are applied. These detection terminologies are further divided in three different modes i.e.; Active parameters based, passive parameters based, and hybridization of two or more techniques. In Passive parameter based detection, mostly the voltage, current, and frequency parameters locally available at the coupling bus are employed to detect islanding. Strong non-detect zone (NDZ), however, is one of the main shortcomings of this method. We refer to these load combinations as the NDZ because they frequently result in the failure of observation for islanded site. A steady ongoing lower-frequency injected signal gets monitored with variations incorporated in the observation, the active parameters based active IDT are evaluated. Design complexity with some negative impact on power quality are drawbacks of such procedures. At the bus of coupling point, ROCOF is measured using the phase locked loop (PLL) in [3–5]. Since the IDTs based on ROCOF is sometimes gets vulnerable to many different varying loads, setting a threshold is difficult. The VU-dependent passive IDT can locate islands by calculating the sequences of negative and positive voltages. The discrete fractional Fourier transform was developed and is utilised by many academics [6]. A HID utilising ROCOF over reactive power and d-axis current injection was employed to increase islanding detection time. In a mixed DG environment, this HID performs well [7]. To address the shortcomings of the first two methods, hybrid IDTs were proposed. Hybrid IDTs combine the advantages of active and passive or two passive/active IDTs, increasing their potency. Grid-connected PV systems have made up the majority of installations during the last few decades. Therefore, having solar PV systems that are connected to the grid is necessary to prevent islanding. This research suggests an improved hybrid IDT based on VU and ROCOF. Due to their simplicity of execution and lack of impact on power quality or detection time, the two PIDs are combined. According to the literature survey, some hybrid IDTs are: In [8] variation in reactive power with Q-f droop analysis; signal processing with controlling by power loop control [9]; voltage phase angle gets evaluated with observing the unbalance in voltages [10]; neural network based performance with wavelet transformations [11]; shift attaining voltage and actual real utilizing power [12]; changes observed by rate in frequency gets observed with sandia shift of frequency [13]; neural networking probabilistically with transformations employing wavelet packets [14]; interfacing the grid network system adaptive with neuro fuzzy [15, 16] analyze the factor of unbalancing in voltage patterns; rate of changes incorporated with reactive and active powers [17]; recognizing the patterns [18]; This paper suggests a combined hybrid improved solution with conclusive VU-ROCOF IDT.

With the combined evaluation of such two locally voltage frequency based available algorithms are merged which further have an additional advantage over no-effect on system-power quality concerns with detection time.

### 1.1 Prevailing Islanding Technique (PIT)

Before based on the imbalance found in the voltage profile and frequency set points in this paper, a recently developed method has been employed to enhance hybrid IDTs. The VU is measured for each DG and three-phase voltages seen at DG connected bus terminals are reported using the current IDT. The authors [19] preferred the technique based on imbalance spikes detected in voltage over the one based on THD in their suggested hybrid IDTs due to its great sensitivity to external disturbance. The frequency of the DG drops from 60 to 59 Hz when the recorded spike of unbalanced voltage exceeds the limit threshold value, which is communicated using the hybrid technique. Continuous voltage frequency measurements are made from the DG output. If the frequency drops below 59.2 Hz within 1.5 s of the shift, the circuit breaker at PCC trips, disconnecting the microgrid from the main grid. The hybrid technique sends a signal to the DG's frequency setpoint, forcing the frequency to drop from 60 to 59 Hz, if the recorded  $V_u$  spike exceeds the threshold value. The DG output voltage's frequency is continuously observed. A trip signal is sent to the circuit breaker at PCC to cut off power to the microgrid if the frequency drops to 59.2 Hz within 1.5 s of the shift. To enable the microgrid to operate on its own, the frequency setpoint is set at 60 Hz. Even after lowering the frequency setpoint to 59 Hz, the frequency at the DG terminal voltage stays near to 60 Hz. The conclusion that islanding has never occurred can be reached. This common strategy is explained using a flowchart in Fig. 1.

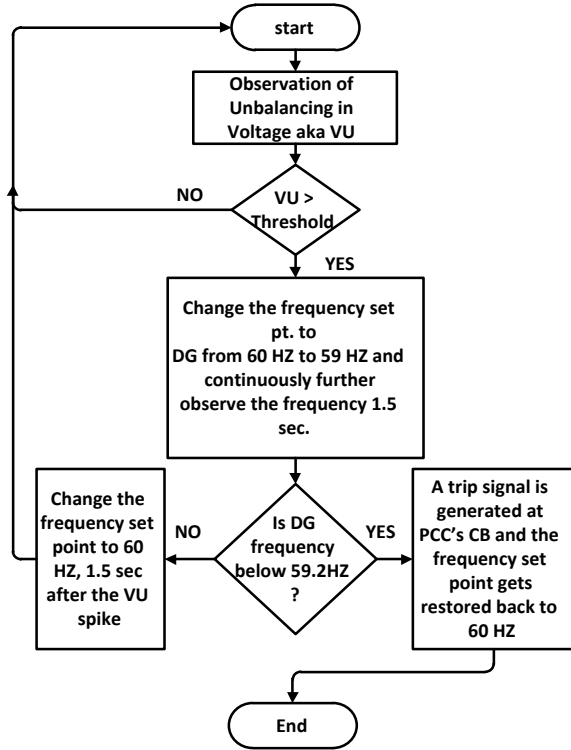
## 2 Proposed technique

The HID that is suggested combines the ROCOF and VU methodologies. In the event of a main grid separation, the DGs installed on the microgrid must be able to handle the load requirements. As a result, voltage imbalances are apparent at the DG terminals. Each DG's VU is measured, and voltage of all three phases gets scrutinize at the DG terminals. Any disturbances, like a sudden shift in the load or a main grid failure, could be detected as an increase in VU. The three-phase voltage imbalance at PCC is described using this PID method, which depends on the VU. This process is known as islanding, and it measures the ratio of the negative sequenced voltage (NSV) to the positive sequence voltage (PSV). The expression below in Eq. (1) can be used to calculate the voltage unbalance at any moment  $t$ .

$$VU_t = \frac{V_{NSt}}{V_{PS_t}} \quad (1)$$

The voltage components in the negative and positive order at the DG output port are displayed. Only when the device is connected to ground do the zero sequence

Fig. 1 PIT chart



components appear. With the calculation of sequence analyzer based Positive, Negative, and Zero components for voltage and current sequence at PCC are evaluated. There are negative sequence components throughout the islanding process [20]. The sequences for voltages given using the expression below in Eqs. (2, 3, 4).

$$V_{a1} = \frac{1}{3}(V_a + \alpha V_b + \alpha^2 V_c) \tag{2}$$

$$V_{a2} = \frac{1}{3}(V_a + \alpha^2 V_b + \alpha V_c) \tag{3}$$

$$V_{a0} = \frac{1}{3}(V_a + V_b + V_c) \tag{4}$$

Va0, Va1, and Va2 represents the zero, positive, and negative series voltages, respectively [21]. Where  $\alpha = 1\angle 120^\circ$ . The ROCOF approach was used to differentiate between the load shift and the mains power failure. Once the VU spike following islanding surpasses a certain threshold, the ROCOF relay tracks the degree of changing frequency for the subsequent 2–50 cycles before transmitting it to the low pass filter (LPF) circuit. LPF is used to lessen high-frequency transients caused

by devices connected to the power system. The threshold value (TV) for a VU spike is 35 times the VU’s average value over the just-past second [19]. After numerous simulations, an empirical decision was made to use a one-second duration. If the length is too short, it may be difficult to identify the spikes since the average values that were produced closely resemble the instantaneous values. Only when instantaneous readings are much higher than average levels may spikes be recognised. If the span is excessively lengthy, such as if an electronically controlled load is applied, there would be an immediate increase in VU. On the other hand, it will take some time for the average value to rise to a greater level. As a result, even a slight surge could cause false tripping. The ROCOF,  $df/dt$ , is recorded across several cycles at the PCC. The circuit breaker can cut off the power output if the  $df/dt$  value is higher than the TV. The ideal TV for the ROCOF approach, according to the literature, is 0.3 Hz/s with 0.7 s for islanded mode limits of detection. ROCOF can be determined [3], using Eq. (5).

$$\frac{df}{dt} = \frac{f(t_k) - f(t_k - \Delta t)}{\Delta t} \tag{5}$$

where  $f(t_k)$  is the frequency at the time of the  $k$ th sample,  $f(t_k - \Delta t)$  is the frequency value determined before the time of the  $k$ th segment, i.e.  $t_k - \Delta t$ . If ROCOF continues to exceed the TV, a trip signal is delivered to the circuit breaker of PCC. Figure 2a displays the flowchart for the suggested approach.

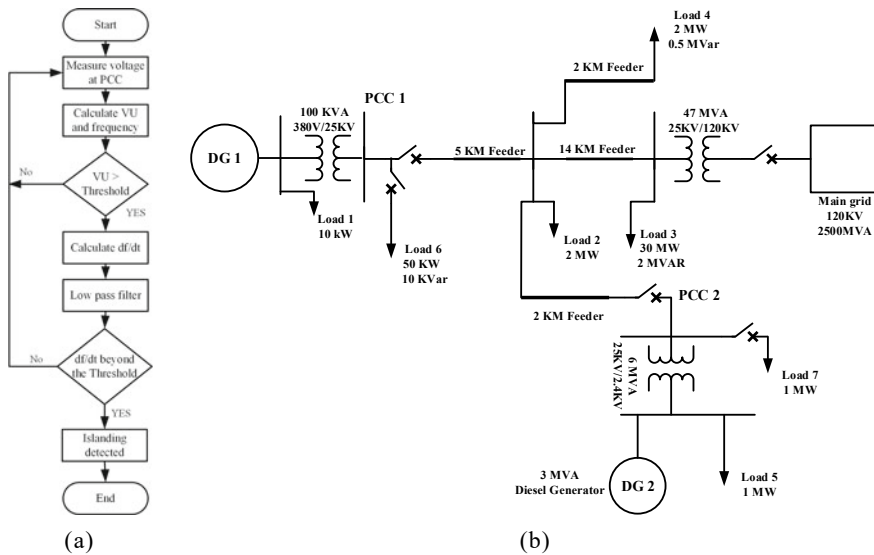
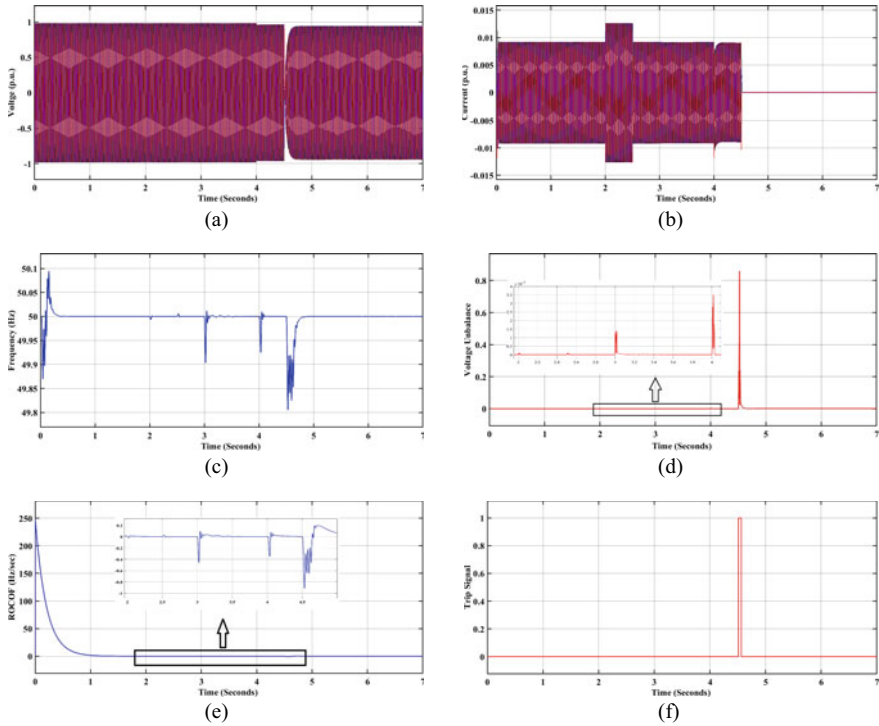


Fig. 2 a Proposed technique’s flow chart, b single line diagram for test system

### 3 Simulation Results

The suggested method has been tested on the test system shown in Fig. 2b. In order to connect a 10 KW PV (DG1) array to a 25 kV feeder at PCC1, a universal bridge and 100 KVA 380 V/25 kV star-delta transformer are utilised. At PCC2, a 3 MVA Synchronous Diesel Generator (DG2) is connected to a 25 kV feeder using a 6 MVA, 25/2.4 kV star-delta transformer. The lengths of four feeder systems are respectively 14 km, 5 km, 2 km, and 2 km, with a combined total of 25 kV. Start the simulation. A 47 MVA 120/25 kV star-delta transformer connects this 25 kV feeder to a 120 kV and 2500 MVA short circuit level main grid. The PV system used was 10 KW. Standard test conditions of 25°C and 1000 W/M<sup>2</sup> are used to launch the simulation. Several disturbances were caused in the PCC1 lab, including 50 kW at 10 kVAR Microgrid 1's (MG1) load number six turns on after two seconds and shuts off after 2.5 s. Switching a 1 MW load 7 in the microgrid 2 at PCC2 at  $t = 3$  s (MG2). At time  $t = 4$  s, Microgrid 2 (MG2) is unplugged. These disruptions result in VU spikes and frequency changes at the corresponding DG terminals. The main grid terminal's circuit breaker opens at  $t = 4.5$  s, which leads to unintentional islanding. A VU spike and ROCOF are thus seen at the terminals of both DGs. Figure 3a–f depicts the results of simulation for the above system at PCC1 (25 kV, 10 MVA base value).

At  $t = 2$ –2.5 s, load 6 in MG1 is shifted, but as can be seen in Figs. 3 and 4, this transition does not significantly affect the loading of DG1 and DG2 (d, e). Because they fall below the limit established by Eq. (1), spike prompt of VU and RO-COF detected by DG1 with DG2 are disregarded. At  $t = 3$  s, MG2 switches to load 7. The loading for both DG-1 and DG2 will not get effected by this change-over. As a result, the VU spike displayed by DG1 and DG2 is observed less than the value and is once again disregarded. The changes are only visible in ROCOF, but the recommended technique does not classify them as accidental islanding. MG2 is deleted with primary grid at  $t = 4$  s. The transition causes a ROCOF spike and a VU spike in PCC1. As demonstrated in Fig. 3, at PCC1, the ROCOF spike reaches the TV but the VU does not (d, e). This implies that the recommended algorithm would not see unintended islanding (UI) as occurring even the microgrid gets disconnected from the central main-grid for repair. UI occurs as a result of the main grid terminal's circuit breaker (C.B.) opening at  $t = 4.5$  s. As a result, the unexpected VU surge occurred at PCC1, as seen in Fig. 3d. Additionally, as seen in the Fig. 3e and f, the ROCOF surpasses the threshold value, causing a trip signal to be transmitted to PCC1 at  $t = 4.515$  s. Islanding may therefore be efficiently monitored in a short amount of time (about 15 ms). The lab at PCC2 had the following disruptions: In microgrid 1 (MG1), load 6 (10 kVAR, 50 kW) switches on after 2 s and shuts off after 2.5 s. Switching a 1 MW load 7 in microgrid 2 at PCC2 at  $t = 3$ –3.5 s (MG2). At  $t = 4$  s, Microgrid 1 (MG1) is unconnected. These disruptions result in spikes and disturbances for VU and frequency respectively at the corresponding DGs. The main grid terminal's circuit breaker opens at  $t = 4.5$  s, which causes UI. A VU spike and ROCOF are thus seen at the terminals of both DGs. The simulation output for the mentioned system at PCC2 (25 kV, 10 MVA base value) is shown in Fig. 4a–f.



**Fig. 3** PCC1 results, **a** voltage(v) (V) (in p.u.) versus time (T) (in sec), **b** current (I) (in p.u.) versus T (in sec), **c** frequency (F) (in Hz) versus T, **d** VU w.r.t T, **e** ROCOF w.r.t T, **f** trip signal indication to PCC-1 station’s CB

As seen in Fig. 4, when load 6 in MG1 is switched at  $t = 2-2.5$  s, it has no discernible impact on the loading of DG1 and DG2 (d, e). Due to the fact that they are below the TV established by equation, the VU spike and ROCOF that DG1 and DG2 detected are ignored (1). At  $t = 3-3.5$  s, MG2 switches to load 7. This changeover does not substantial impact on the load charging distribution for DG-1 and DG2. Thereafter, the spike for the VU is visualized at DG1 and DG2 station which will be below the control value that resulted in disregarded once again. The changes are only visible in ROCOF, but the recommended technique does not classify them as UI. MG-1 gets obsoleted from the grid at  $t = 4$  s. The transition causes a ROCOF spike and a VU spike in PCC2. At PCC2, as demonstrated in Fig. 4, ROCOF and VU spikes do not exceed the TV (d, e). This is predicated on the notion that the approach not take UI into account, even microgrid were isolated from the main grid for maintenance. UI occurs when the main grid terminal’s circuit breaker (C.B.) opens at  $t = 4.5$  s. As a result, PCC2 saw the unanticipated VU increase, as illustrated in Fig. 4d. A trip signal is provided to PCC 2 at  $t = 4.517$  s as a result of the ROCOF exceeding the threshold value in the Figs. 4e and f, respectively. Therefore, islanding may be efficiently seen in a short amount of time (about 17 ms).

### 4 Conclusion

This study provides a unique HID approach for microgrids with inverter-based diesel generators employing VU and ROCOF.

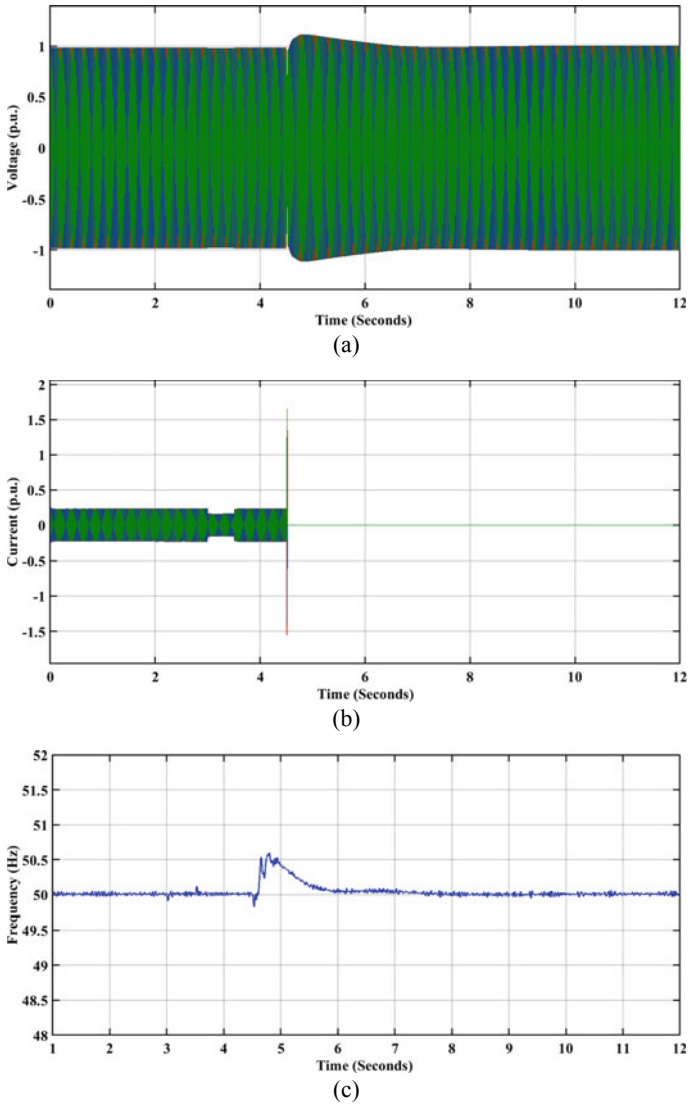


**Fig. 4** PCC-2's results at, **a** V (in p.u.) versus T (in sec.), **b** I (in p.u.) versus T, **c** F (Hz) versus T, **d** VU w.r.t T, **e** ROCOF w.r.t T, **f** trip signal indication generated at PCC-2's station CB



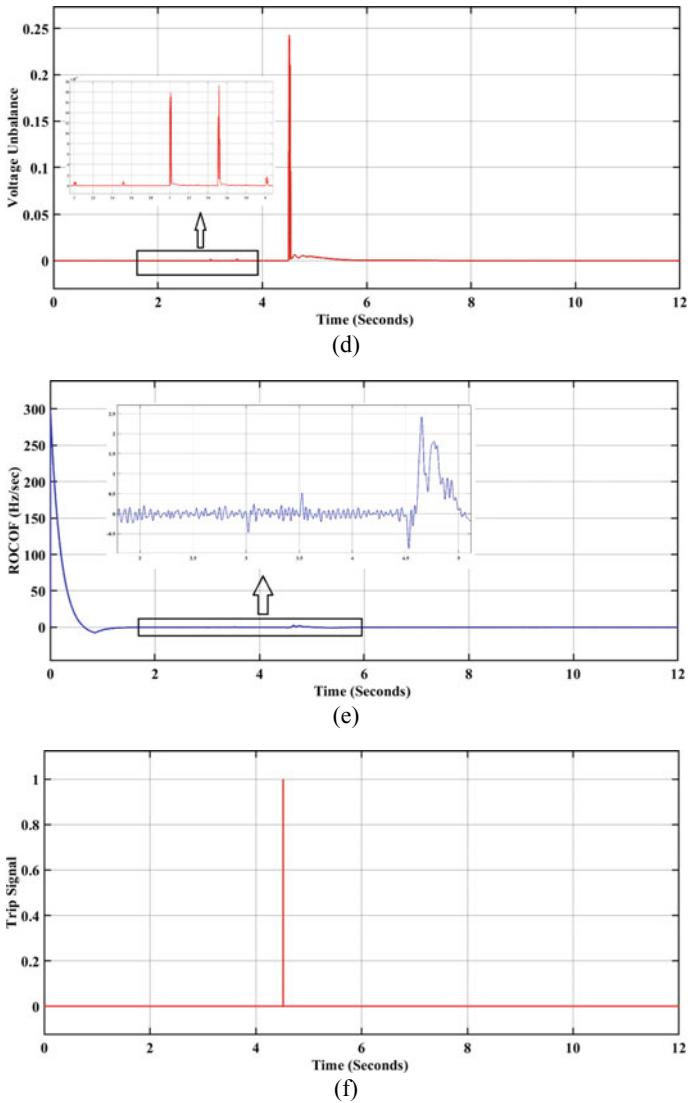


Fig. 4 (continued)

The proposed hybrid approach is contrasted with the hybrid IDT based on the literature’s frequency setpoint (FSP) and VU. This technique can distinguish between islanded situations and load switching conditions, preventing spurious trips in the event of load switching. When used with a multi-DG system, this method works as intended. As a result, the suggested IDT performs better than PID methods with huge NDZ and active methods with poor power quality and no potential for autonomous operation in islanded mode. According on the simulation results, the suggested hybrid

method's islanding detection time is between 15 and 25 ms. The hybrid approach employing VU and frequency setpoint was also shown to have an islanding detection time of 0.21 s. MATLAB/Simulink is used to produce the simulation results.

## References

1. Wang G (2020) Design consideration and performance analysis of a hybrid islanding detection method combining voltage unbalance/total harmonic distortion and bilateral reactive power variation. *CPSS TPEA* 5:86–100
2. Rawat MS, Vadhera S (2021) Evolution of islanding detection method for microgrid systems. *Adv Comput Electric Eng* 221–257
3. Marchesan G, Muraro MR, Cardoso G et al (2016) Passive method for distributed-generation island detection based on oscillation frequency. *IEEE Trans Power Deliv* 31:138–146
4. Guha B, Haddad RJ, Kalaani Y (2015) A passive islanding detection approach for inverter-based distributed generation using rate of change of frequency analysis. *Southeast Con*
5. Tzelepis D, Dysko A, Booth C (2016) Performance of loss-of-mains detection in multi-generator power Islands. In: 13th international conference on development in power system protection 2016 (DPSP)
6. Dutta S, Olla S, Sadhu PK (2021) A secured, reliable and accurate unplanned island detection method in a renewable energy based microgrid. *Eng Sci Technol Int J* 24:1102–1115
7. Nougain V, Prakash S, Mishra S (2018) Hybrid islanding detection method based on ROCOF over reactive power and d-axis current injection. In: 2018 8th IEEE India international conference on power electronics (IICPE)
8. Raipala O, Makinen A, Repo S, Jarventausta P (2014) A novel anti-islanding protection method based on the combination of a Q-f droop and RPV. In: IEEE PES innovative smart grid technologies. Europe IEEE, pp 1–6
9. Zamani R, Hamedani Golshan ME, Haes Alhelou H, Hatziargyriou N (2019) A novel hybrid islanding detection method using dynamic characteristics of synchronous generator and signal processing technique. *Electric Power Syst Res* 175:105911
10. Seyedi M, Taher SA, Ganji B, Guerrero JM (2019) A hybrid islanding detection technique for inverter-based distributed generator units. *Int Trans Electr Energy Syst* 29
11. Kumar SA, Subathra MSP, Kumar NM et al (2020) A novel Islanding detection technique for a resilient photovoltaic-based distributed power generation system using a tunable-Q wavelet transform and an artificial neural network. *Energies* 13:4238
12. Mahat P, Chen Z, Bak-Jensen B (2009) A hybrid Islanding detection technique using average rate of voltage change and real power shift. *IEEE Trans Power Deliv* 24:764–771
13. Khodaparastan M, Vahedi H, Khazaeli F, Oraee H (2017) A novel hybrid islanding detection method for inverter-based DGs using SFS and ROCOF. *IEEE Trans Power Deliv* 32(5):2162–2170
14. Ahmadipour M, Hizam H, Lutfi Othman M, Amran Mohd Radzi M (2018) An anti-Islanding protection technique using a wavelet packet transform and a probabilistic neural network. *Energies* 11:2701
15. Hashemi F, Ghadimi N, Sobhani B (2013) Islanding detection for inverter-based DG coupled with using an adaptive neuro-fuzzy inference system. *Int J Electr Power Energy Syst* 45:443–455
16. Nayak AM, Mishra M, Pati BB (2020) A hybrid islanding detection method considering voltage unbalance factor. In: 2020 IEEE international symposium on sustainable energy, signal processing and cyber security (ISSSC). IEEE, pp 1–5
17. Jhuma UK, Mekhilef S, Mubin M et al (2021) Hybrid islanding detection technique for distribution network considering the dynamic behavior of power and load. *Circuit Theory Apps* 50:1317–1341

18. Marín-Quintero J, Orozco-Henao C, Velez JC, Bretas AS (2021) Micro grids decentralized hybrid data-driven cuckoo search based adaptive protection model. *Int J Electr Power Energy Syst* 130(106960):106960
19. Menon V, Nehrir MH (2007) A hybrid islanding detection technique using voltage unbalance and frequency set point. *IEEE Trans Power Syst* 22:442–448
20. Kumar KM, Naresh M, Singh NK, Singh AK (2016) A passive islanding detection approach for distributed generation using rate of change of negative sequence voltage and current. In: 2016 IEEE Uttar Pradesh section international conference on electrical, computer and electronics engineering (UPCON)
21. (2018) An efficient passive islanding detection method for integrated DG system with zero NDZ. *IJRER*